Published December 20, 2004

Interdependent assembly of specific regulatory lipids and membrane fusion proteins into the vertex ring domain of docked vacuoles

Rutilio A. Fratti, Youngsoo Jun, Alexey J. Merz, Nathan Margolis, and William Wickner

Department of Biochemistry, Dartmouth Medical School, Hanover, NH 03755

Membrane microdomains are assembled by lipid partitioning (e.g., rafts) or by protein–protein interactions (e.g., coated vesicles). During docking, yeast vacuoles assemble "vertex" ring-shaped microdomains around the periphery of their apposed membranes. Vertices are selectively enriched in the Rab GTPase Ypt7p, the homotypic fusion and vacuole protein sorting complex (HOPS)–VpsC Rab effector complex, SNAREs, and actin. Membrane fusion initiates at vertex microdomains. We now find that the "regulatory lipids" ergosterol, diacylglycerol and 3- and 4-phosphoinositides accumulate at vertices in a mutually interdependent manner. Regulatory lipids are also required for the vertex enrichment of SNAREs, Ypt7p, and HOPS. Conversely, SNAREs and actin regulate phosphatidylinositol 3-phosphate vertex enrichment. Though the PX domain of the SNARE Vam7p has direct affinity for only 3-phosphoinositides, all the regulatory lipids which are needed for vertex assembly affect Vam7p association with vacuoles. Thus, the assembly of the vacuole vertex ring microdomain arises from interdependent lipid and protein partitioning and binding rather than either lipid partitioning or protein interactions alone.

Introduction

Membrane fusion is catalyzed by conserved factors (Jahn and Sudhof, 1999), including Rab family GTPases and their effectors (Chavrier and Goud, 1999), SNAREs (Gerst, 1999), chaperones such as NSF (Sec18p), α-SNAP (Sec17p), and SM proteins (Fasshauer et al., 1997; Jahn, 2000), and phosphoinositides (Mayer et al., 2000; Boeddinghaus et al., 2002). The functional relationships among the proteins and lipids at fusion-competent microdomains are unknown.

Vacuolar homotypic fusion in *Saccharomyces cerevisiae* uses the same mechanisms as other fusion reactions (Wickner and Haas, 2000). Recent studies reveal a novel spatial arrangement of proteins on docked vacuoles (Wang et al., 2002). Clustered vacuoles have three membrane subdomains. Regions of membrane not in contact with other vacuoles are the "outside" membrane. Docked vacuoles have two flat disc regions of tightly apposed membranes which are called the "boundary" membrane. The ring-shaped periphery of the boundary membrane is termed the "vertex". The vertex is enriched with regulators of vacuole fusion including the Rab Ypt7p, SNAREs, homotypic fusion and vacuole protein sorting complex (HOPS), and actin (Eitzen et al., 2002; Wang et al., 2002, 2003). Fusion occurs around the vertex, internalizing boundary membrane (Wang et al., 2002). Rabs and SNAREs also localize to membrane microdomains in other fusion systems (TerBush et al., 1996; Roberts et al., 1999; Guo et al., 2001; Lang et al., 2001).

Vacuole fusion occurs in ordered subreactions. During priming, Sec17p-bound cis SNARE complexes are disassembled by Sec18p, releasing both Sec17p (Mayer et al., 1996) and the soluble SNARE Vam7p (Boeddinghaus et al., 2002). Vam7p reassociates with vacuoles via its interactions with Ypt7p (Ungermann et al., 2000) and with phosphatidylinositol (PI) 3-phosphate (PI(3)P) through its PX domain (Cheever et al., 2001; Boeddinghaus et al., 2002). Docking is initiated by Ypt7p-dependent tethering, followed by vertex ring assembly. Docking requires Ypt7p/GTP, HOPS (Price et al., 2000), Rho GTPases (Eitzen et al., 2001; Muller et al., 2001), and actin remodeling (Eitzen et al., 2002). Actin remodeling is also regulated by phosphoinositides (Higgs and Pollard, 2000; Rozelle

Correspondence to Bill Wickner: Bill.Wickner@dartmouth.edu

A.J. Merz's current address is Dept. of Biochemistry, University of Washington, Seattle, WA 98195

Abbreviations used in this paper: 3NC, 3-nitrocoumarin; ENTH, epsin NH_2-terminal homology domain; HOPS, homotypic fusion and vacuole protein sorting complex; LatB, latrunculin B; MED, MARCKS effector domain; PI, phosphatidylinositol; PI(3)P, PI 3-phosphate; PX, Phox homology.

The Journal of Cell Biology, Vol. 167, No. 6, December 20, 2004 1087–1098
http://www.jcb.org/cgi/doi/10.1083/jcb.200409068

Published December 20, 2004

et al., 2000). Late stages of vacuole fusion may be mediated by SNAREs (Nichols et al., 1997; Fukuda et al., 2000), calmodulin (Peters and Mayer, 1998), protein phosphatase 1 (Peters et al., 1999), V_0 complex (Peters et al., 2001), Vtc complex (Muller et al., 2003), Vac8p (Wang et al., 2001c), actin (Eitzen et al., 2002) and phosphoinositides (Mayer et al., 2000).

Lipids have specific roles in vacuole fusion. Ergosterol, a yeast sterol, regulates Sec17p release during priming (Kato and Wickner, 2001). At least two phosphoinositides regulate fusion. PI(3)P recruits Vam7p to vacuoles (Cheever et al., 2001; Boeddinghaus et al., 2002), and cells lacking PI 3-kinase have fragmented vacuoles (Seeley et al., 2002). PI(4,5)P_2 also regulates vacuole fusion (Mayer et al., 2000), although by undefined means. PI(4,5)P_2 may regulate actin remodeling (Rozelle et al., 2000), which is required for vertex ring assembly (Wang et al., 2003) and fusion (Eitzen et al., 2002).

We have now examined lipid spatial distributions on docked vacuoles and the relationships between regulatory lipids and vertex-enriched fusion proteins. Fluorescent lipid ligands were used to probe the distribution of PI(3)P, PI(4,5)P_2, ergosterol, and DAG. These "regulatory lipids" become enriched at vertices during docking. Antagonists of actin remodeling and SNARE function modified the distribution of PI(3)P, whereas selective sequestration or enzymatic depletion of regulatory lipids altered the vertex enrichment of other lipids and of SNAREs, Ypt7p, and HOPS. Thus, lipids and proteins are interdependent for the assembly of a complex membrane docking junction where fusion occurs.

Results

Vacuole fusion requires PI(3)P (Boeddinghaus et al., 2002), PI(4,5)P_2 (Mayer et al., 2000), ergosterol (Kato and Wickner, 2001), and DAG (Jun et al., 2005). We now use specific lipid-binding ligands for two different purposes, at either inhibitory concentrations (Fig. 1, closed arrows) or, for probing lipid localization, at subinhibitory concentrations (Fig. 1, open arrows).

To probe PI(3)P, we use a tandem FYVE domain which specifically binds PI(3)P (Gillooly et al., 2000). At high concentrations, FYVE inhibits Vam7p reassociation with the vacuole (Boeddinghaus et al., 2002). FYVE domain derivatized with the fluorophore Cy3 does not inhibit vacuole fusion at 0.2 μM (Fig. 1 A). This concentration was used to monitor PI(3)P localization. To probe PI(4,5)P_2, we used MARCKS effector domain (MED; Wang et al., 2001a) and an epsin NH_2-terminal homology domain (ENTH; Rosenthal et al., 1999). MED and ENTH inhibited vacuolar fusion at 8 and 30 μM (Fig. 1, B and C), consistent with the requirement for PI(4,5)P_2 for vacuole fusion (Mayer et al., 2000). These ligands showed little inhibition at the low concentrations used for labeling. DAG was probed with 1 μM Alexa488-tagged C1b domain (Fig. 1 D; Johnson et al., 2000). At higher concentrations (10 μM), C1b blocked vacuole fusion (Fig. 1 D). Fusion is blocked by 19 μM filipin (Kato and Wickner, 2001), an intrinsically fluorescent ergosterol ligand (Fig. 1 E). Like the other ligands, filipin was used at a subinhibitory concentration for labeling. As a probe for phosphatidylserine (PS), which is not required for vacuole fusion (Mayer et al., 2000), we used the fluor PSS-380 (Koulov et al., 2003) which did not affect vacuole fusion (Fig. 1 F). The role of regulatory lipids was further established using lipid-modifying enzymes. MTM-1 hydrolyzes the D3 phosphate of PI(3)P (Taylor et al., 2000), and SigD hydrolyzes the 5′-phosphate of PI(4,5)P_2 (Marcus et al., 2001). They are potent inhibitors of fusion (Fig. 1, G and H).

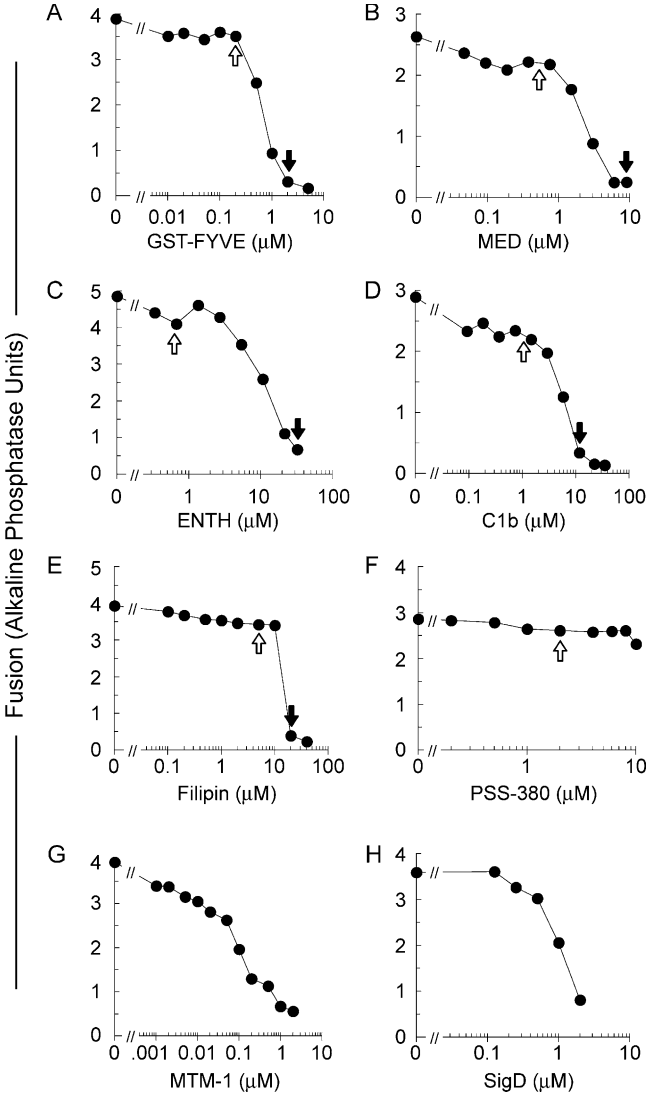

Figure 1. **Ligands and enzymes which target phosphoinositides, DAG and ergosterol inhibit vacuole fusion.** Fusion reactions with vacuoles from BJ3505 and DKY6281 were performed in the absence or presence of the indicated concentrations of GST-FYVE (A), MED (B), ENTH (C), C1b (D), Filipin (E), PSS-380 (F), MTM-1 (G), or SigD (H), added from the start of the reaction. Fusion was assayed by phosphatase activity and expressed in U. Closed arrows indicate inhibitory concentrations used in this study. Open arrows indicate sub-inhibitory concentrations used for determining lipid localization.

Even high levels of these lipid ligands do not prevent Ypt7p-dependent tethering (Fig. 2). To assay tethering (Mayer and Wickner, 1997; Wang et al., 2002), vacuoles were incubated with ATP for 30 min to allow docking into

Published December 20, 2004

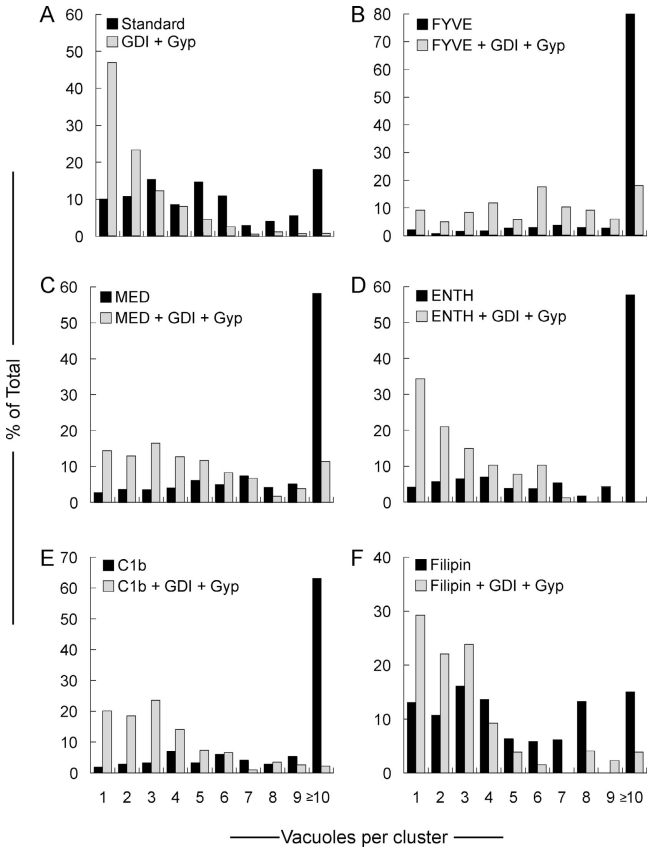

Figure 2. **Regulatory lipids are not required for Ypt7p-dependent tethering.** For quantitative microscopic assay of docking (Mayer and Wickner, 1997), vacuoles were incubated with PS buffer or treated with 2.8 μM Gdi1p and 11.4 μM Gyp1-46p for 10 min at 27°C in the absence of ATP. Aliquots were then added to chilled tubes containing docking buffer, 2 μM GST-FYVE, 10 μM MED, 30 μM ENTH, 10 μM C1b or 19 μM filipin. Reactions were supplemented with the docking reaction ATP-regenerating system and returned to 27°C for 20 min. After incubation, docking reactions were placed on ice, incubated for 2 min with FM4-64 and mounted on slides for analysis. For each condition, 10 random fields were scored for cluster size. Vacuole clusters (A, black bars) include some vacuoles of enlarged diameter, reflecting fusion (not depicted).

clusters. Random microscopic fields were photographed and scored for vacuoles per cluster. Though most vacuoles participate in cluster formation (Fig. 2 A, black bars), clustering was blocked by Ypt7p extraction by Gdi1p, aided by the GAP Gyp1-46 (gray bars). Vacuole docking is followed by fusion, lowering the number of vacuoles per cluster; thus this assay only provides a minimal estimate of docking. Blocking fusion by lipid ligands enhances the number of vacuoles per cluster (Fig. 2 B-E, black bars). Nevertheless, this is authentic docking as it is blocked by Ypt7p extraction. Filipin inhibits at multiple stages of the vacuole fusion pathway including priming (Kato and Wickner, 2001), and this parallel slowing of each reaction stage yielded a distribution of vacuoles per cluster (Fig. 2 F) that resembled the uninhibited reaction (Fig. 2 A). The clustering of filipin treated vacuoles was still inhibited by inactivation of Ypt7p. Thus, we used lipid ligands to quantify the distribution of relevant proteins and lipids on vacuoles which were tethered via the physiological pathway.

Selective lipid enrichment at vertices of docked vacuoles

Because SNAREs, Ypt7p, HOPS, and actin become enriched at vertices (Eitzen et al., 2002; Wang et al., 2002, 2003), we examined the distribution of regulatory lipids by monitoring the distribution of fluorescent lipid-specific probes on docked vacuoles. Cy3-FYVE labeling shows that PI(3)P is enriched at many vertices (Fig. 3, C and D). Similarly, Cy3-ENTH (Fig. 3, F and G), filipin (Fig. 3, I and J), and Alexa488-C1b (Fig. 3, L and M) were concentrated at vertices. While the lipids required for vacuole fusion are enriched at vertices, PS is evenly distributed (Fig. 3, O and P), as are the nonspecific dyes MDY-64 (Fig. 3, B and E) and FM4-64 (Fig. 3, H, K, and N).

To quantify regulatory lipid enrichment, we used ratiometric fluorescence microscopy (Wang et al., 2002, 2003), comparing the concentration of each lipid at vertex sites to either FM4-64 or MDY-64. The specific-to-nonspecific probe ratios were normalized to yield a mean value of 1 at the outside membrane of docked vacuoles. Consequently, the values for boundary and vertex sites indicate enrichment or depletion of specific lipids with respect to the outside membrane (Wang et al., 2002). Ratio values were determined at every vertex, boundary midpoint, and outer membrane midpoint for over 10 clusters of docked vacuoles. The ratiometric assay (Wang et al., 2002, 2003) shows 1.2–4-fold mean lipid and protein enrichment at vertices. These are lower bounds estimates of the enrichments for three reasons. First, the variability among vertex sites reflects the asynchrony of vertex assembly. Fully mature vertex sites may be closer to fusion, and hence have shorter half-lives, than partially assembled sites. This is underscored by the finding (Fig. 6 B, below) that late fusion stage inhibitors yield dramatically higher vertex enrichment values. Second, vertices may be below the diffraction limit. Third, relatively low levels of fluorescence are obtained, particularly with GFP-tagged proteins expressed under native promoters. Each of these factors increases the noise level (Inoue and Spring, 1997) and thereby attenuates the maximal observed enrichment values. Notably, other studies of SNARE (Lang et al., 2001) and Rab GTPase (Roberts et al., 1999) localization during docking in mammalian cells have reported mean enrichments of approximately twofold, similar to our values. Each of these measurements provide conservative indices of the actual accumulation at docking sites.

The ratio data for each treatment, probe, and morphological location are shown in cumulative distribution plots where individual measurements are ranked, then each is plotted at its rank percentile (Fig. 4, A–F). Cy3-FYVE, and thus PI(3)P, was enriched at vertices (Fig. 4 A). Similarly, rhodamine-MED and Cy3-ENTH, and thus PI(4,5)P_2, were also vertex enriched (Fig. 4, B and C). Filipin, an ergosterol-binding drug, and Alexa488-C1b, a DAG probe, were also enriched at vertices (Fig. 4, D and E). In contrast, PSS-380 (Koulov et al., 2003) was not enriched at vertex or boundary regions (Fig. 4 F), showing the selectivity of vertex lipid enrichment. In sum, PI(3)P, PI(4,5)P_2, DAG, and ergosterol, but not PS, accumulate at vertex sites. Fig. 4 G shows the geometric means and 95% confidence intervals for these means

Published December 20, 2004

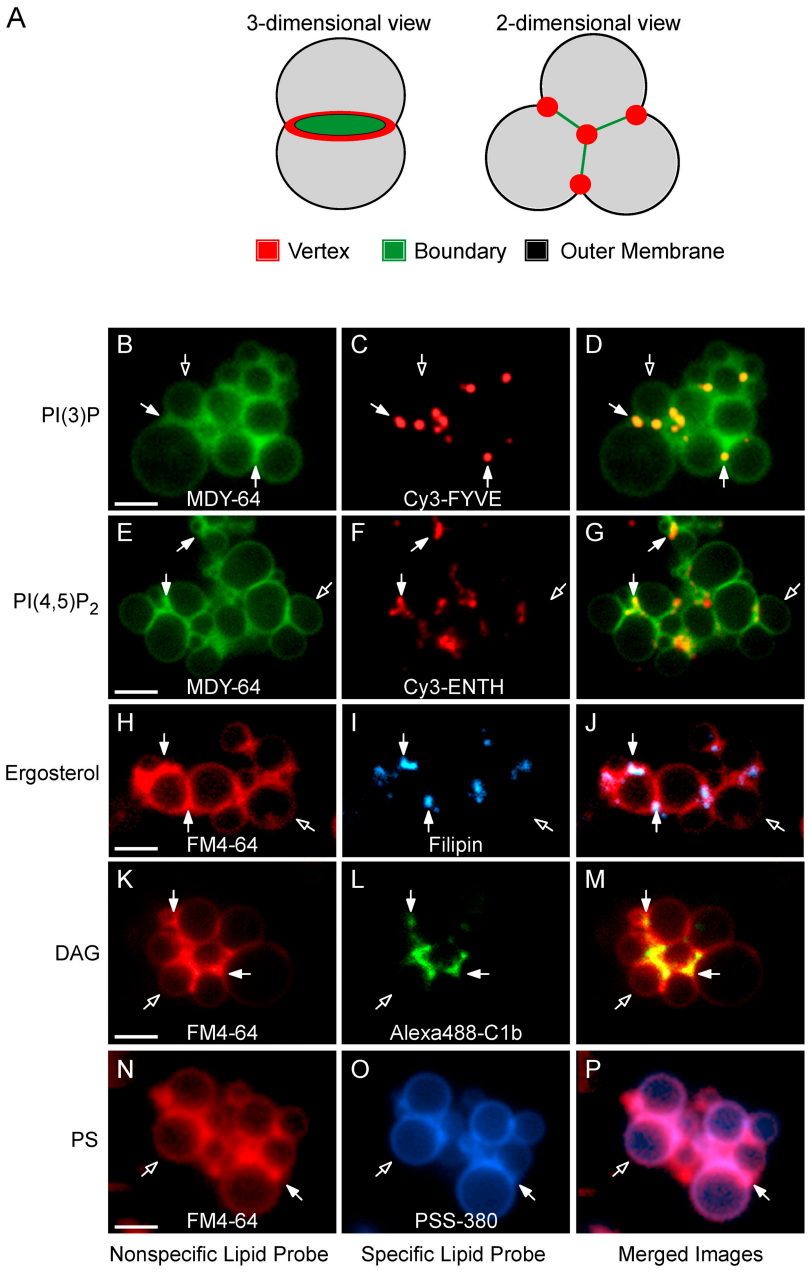

Figure 3. **Lipids are enriched at the vertices of docked vacuoles.** Vacuoles from DKY6281 yeast were incubated under docking conditions for 30 min at 27°C with fluorescent lipid ligands. After incubation, docking reactions were placed on ice and labeled with either FM4-64 or MDY-64. (A) Outer membrane, boundary membrane and vertex ring subdomains of docked vacuoles. (B and E) MDY-64 or (H, K, and N) FM4-64 label the entire membrane. Specific lipids were labeled with (C) 0.2 μM Cy3-FYVE to label PI(3)P, (F) 0.6 μM Cy3-ENTH to label $PI(4,5)P_2$, (I) 5 μM filipin to label ergosterol, (L) 1 μM Alexa488-C1b to label DAG, or (O) 2.5 μM PSS-380 to label PS. For Cy3-ENTH labeling, vacuoles were reisolated (5,220 *g*, 4°C, 5 min) at the end of the 30-min incubation to eliminate background fluorescence from unbound probe and resuspended in the original volume of PS buffer before labeling with MDY-64 and analysis. D, G, J, M, and P show merged images of nonspecific and specific probes. Closed arrows are examples of vertex sites enriched in the specified regulatory lipid. Open arrows are outer membrane microdomains. Bars, 2 μm. As shown below (Fig. 9), ENTH displaces Vam7p from membranes after 90 min under fusion conditions which are different from the docking conditions and time (30 min) used here.

for the data in Fig. 4 (A–F). As shown below, the recruitment of these lipids is subject to complex regulation.

Interdependence of SNAREs and lipids for vertex assembly

We monitored PI(3)P distribution when other vertex-enriched lipids were sequestered by ligands. The addition of C1b, MED, ENTH, or filipin inhibited PI(3)P vertex enrichment ($P < 0.00001$; Fig. 5 A). Lipid ligands also affected ergosterol vertex enrichment. Filipin staining showed that ergosterol was enriched at vertices (Fig. 4, D and G). ENTH blocked ergosterol vertex enrichment ($P < 0.01$; Fig. 5 B), showing that $PI(4,5)P_2$ is required for ergosterol vertex accumulation. In contrast, the PI(3)P ligand PX augmented ergosterol levels at vertices ($P < 0.001$; Fig. 5 B), suggesting either that PI(3)P inhibits ergosterol vertex enrichment or that inhibition of fusion by PX domain prevents fusion-triggered dissociation of assembled vertices. Though MED is bound mainly to $PI(4,5)P_2$ in cells (McLaughlin et al., 2002), it can also bind $PI(3,4)P_2$ (Wang et al., 2001a), PI(4)P (Seki et al., 1996) and PI(3)P (unpublished data). Apparently, the positive effect of MED on ergosterol vertex enrichment (by blocking fusion-induced vertex loss) and the negative effect (through sequestration of $PI(4,5)P_2$) are balanced. C1b only had a minor effect on ergosterol accumulation at vertices, suggesting that DAG is not required for ergosterol enrichment. Though C1b blocked PI(3)P localization to vertices (Fig. 4 A), PI(3)P is presumably not needed for ergosterol enrichment at vertices because ergosterol enrichment is not inhibited by PX domain. These effects could occur directly, through disruption of lipid microdomain architecture, or indirectly through lipid binding proteins such as Vam7p.

Published December 20, 2004

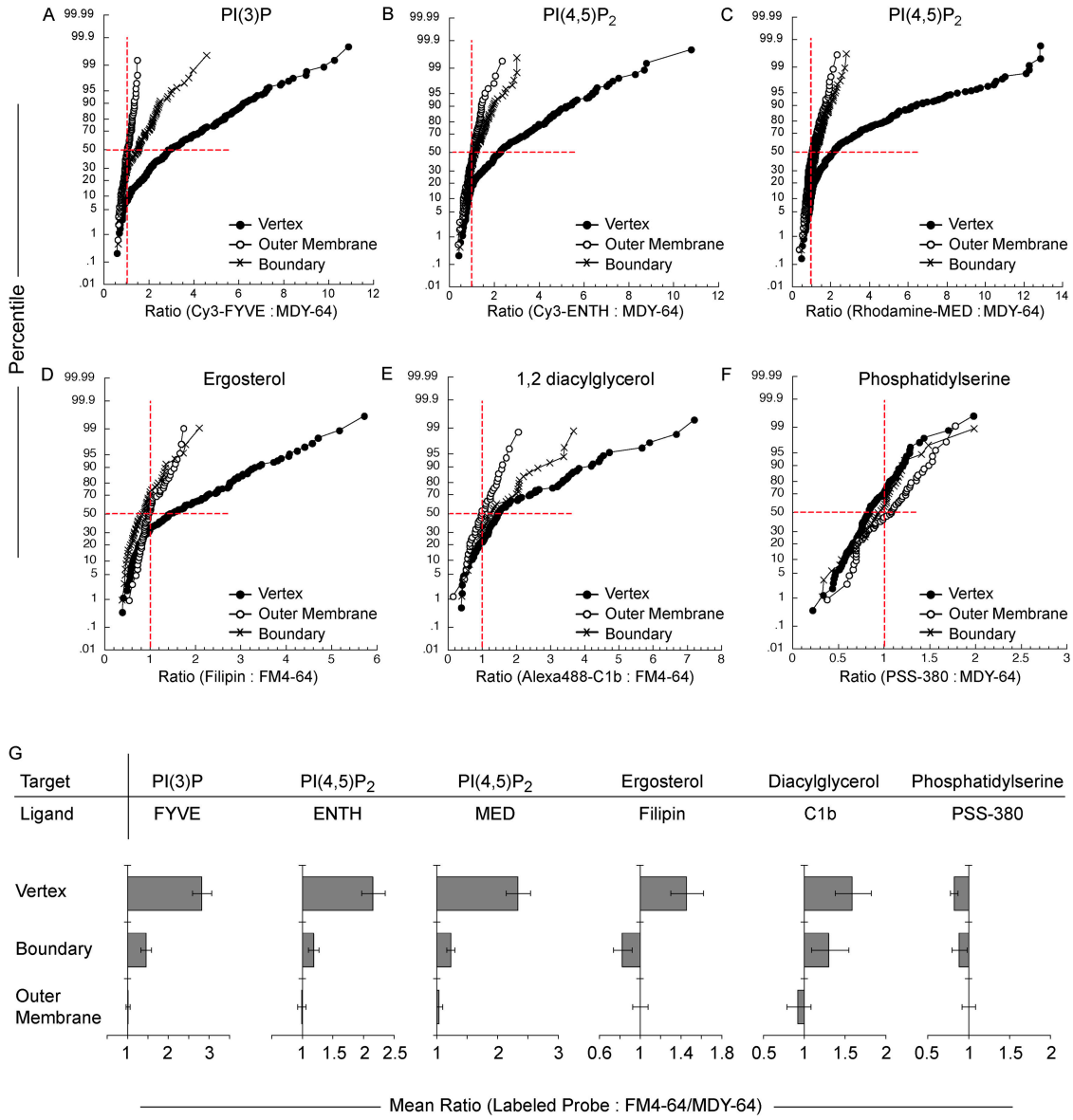

Figure 4. **Quantitation of lipid enrichment at vertices.** Docking reactions were performed as in Fig. 3. After 30 min at 27°C with fluorescent lipid ligands, reactions were placed on ice, labeled with either FM4-64 or MDY-64, and analyzed. Cumulative distribution plots depict the percentile values of each specific lipid ligand/nonspecific lipophilic dye ratio for each of the three microdomains. Each curve is comprised of measurements from ≥10 vacuole clusters where the maximum intensity was determined for every vertex and midpoint of boundary and outer membrane. Intensities were measured in both fluorescence channels at each subdomain and are expressed as a ratios of specific to nonspecific label. Outer membrane ratios were normalized to a value of 1 and the enrichment of specific label at vertices and boundaries were expressed relative to outer membrane intensities. Each ratio in a dataset is ordered and plotted versus the percentile rank of the values. Lipids were labeled with the same concentrations of ligands as in Fig. 3. (G) Geometric means with their 95% confidence intervals for the data from the cumulative distribution plots in A–F.

We next examined whether protein fusion catalysts affect the vertex enrichment of regulatory lipids. To test the effect of SNAREs, we exploited recombinant Sec17p which, at high concentrations, drives unpaired SNAREs into cis complexes (Wang et al., 2000) and competes with HOPS for binding to SNARE complexes (K. Collins, personal communication). Excess Sec17p reduced Cy3-FYVE enrichment at vertices ($P < 0.0001$; Fig. 6 A). This was reversed when excess Sec18p was present (Fig. 6 A), establishing the specificity of Sec17p action. Anti-Vam3p, which blocks SNARE vertex enrichment (Wang et al., 2003), also prevented PI(3)P vertex enrichment ($P < 0.00001$; Fig. 6 A), confirming the role of SNAREs in PI(3)P function.

Actin accumulates at vertices (Eitzen et al., 2002; Wang et al., 2003) and its remodeling is required for SNARE vertex enrichment (Wang et al., 2003). To determine whether actin remodeling affects PI(3)P vertex enrichment, we used drugs to either stabilize F-actin or prevent its formation. Jasplakinolide prevents depolymerization by stabilizing F-actin (Morton et al., 2000) and blocks vacuole fusion (Eitzen et al., 2002). Although jasplakinolide has no effect on the vertex enrichment of Ypt7p (Wang et al., 2003), it reduced Cy3-FYVE vertex enrichment ($P < 0.01$; Fig. 6 B). In contrast, latrunculin B (LatB), which prevents actin polymerization (Ayscough, 2000), increased Cy3-FYVE labeling at vertices ($P < 0.0001$; Fig. 6 B). LatB

Published December 20, 2004

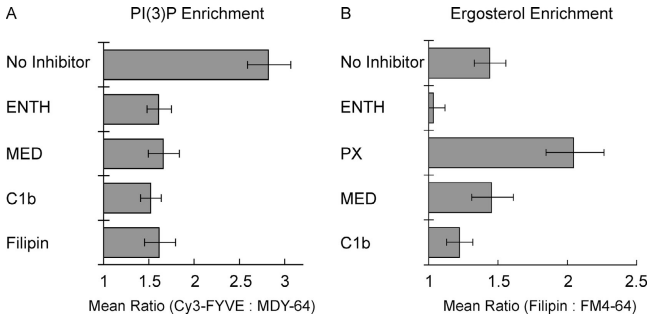

Figure 5. **Interdependence of the vertex enrichment of regulatory lipids.** Docking reactions were labeled with (A) 0.2 μM Cy3-FYVE or (B) 5 μM filipin and incubated with either 30 μM ENTH, 10 μM MED, 10 μM C1b, 19 μM filipin, 25 μM PX, or buffer alone. After 30 min at 27°C, reactions were placed on ice, labeled with MDY-64 (A) or FM4-64 (B), and prepared for fluorescence microscopy. Relative enrichments of specific probes were determined as in Fig. 3. Data are presented as geometric mean values ± 95% confidence intervals of the relative enrichment at vertices.

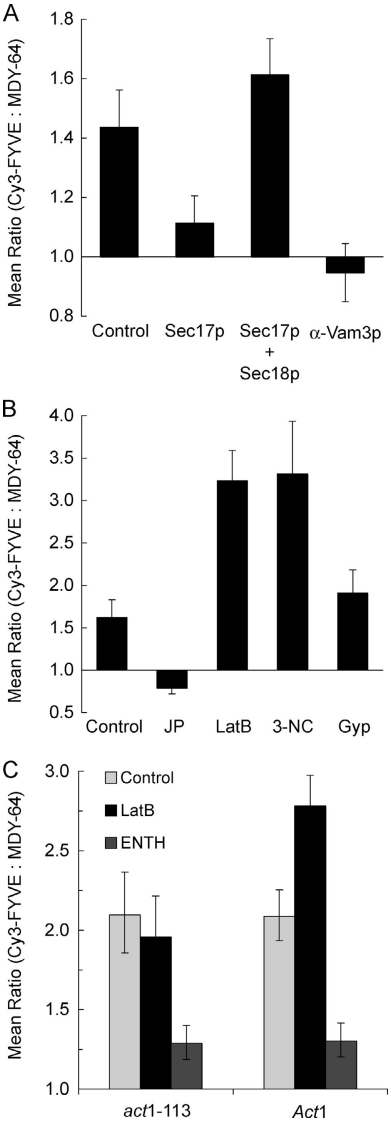

Figure 6. **Protein ligands affect PI(3)P localization.** (A and B) Docking reactions using DKY6281 vacuoles labeled with 0.2 μM Cy3-FYVE (as described in Figs. 2 and 3) were treated with 750 nM (excess) Sec17p, 1.2 μM Sec18p, both excess Sec17p and Sec18p, 190 nM anti-Vam3 F_{ab}, 0.5 mM jasplakinolide, 0.8 mM LatB, 11.4 μM Gyp1-46p (Gyp), or 250 μM 3NC. After 30 min at 27°C, reactions were placed on ice and prepared for fluorescence microscopy. Geometric mean values ± 95% confidence intervals of the relative enrichment at vertices are shown. (C) To determine whether the effects of LatB were due to alterations in actin polymerization, vacuoles were harvested from isogenic DDY182 yeast containing *Act*1 or the latrunculin resistant mutant *act*1-113 and used in docking experiments. Vacuoles were labeled with Cy3-FYVE and incubated during docking reactions with 0.8 mM LatB or 30 μM ENTH where indicated. Samples were prepared and analyzed as in Figs. 2 and 3.

does not alter the vertex enrichment of Vam3p (Wang et al., 2003). Actin depolymerization may promote PI(3)P enrichment at vertices, and repolymerization may either inhibit PI(3)P vertex enrichment or allow its dispersal during fusion. As a control, we tested vacuoles from cells bearing the *act1-113* mutation, which confers resistance to latrunculin (Ayscough et al., 1997), or from isogenic *ACT*1 cells. LatB had no effect on Cy3-FYVE vertex enrichment on *act1-113* derived vacuoles (Fig. 6 C), though it enhanced Cy3-FYVE vertex labeling on vacuoles from the *ACT1* parent strain ($P < 0.0001$; Fig. 6 C), showing that the effects of LatB on PI(3)P were due to alterations in actin polymerization. The vertex enrichment of PI(3)P on docked *ACT1* or *act1-113* vacuoles showed similar responses to other ligands such as ENTH, indicating that the mobilization of PI(3)P to vertices is otherwise unaffected by the *act1-113* mutation.

Although C1b inhibited PI(3)P vertex enrichment, and one pathway to DAG is through hydrolysis of $PI(4,5)P_2$ by PLC, it remained unclear whether PLC activity might affect vertex ring assembly. To address this, we used 3-nitrocoumarin (3NC) to inhibit PLC activity (Tisi et al., 2001). 3NC dramatically increased Cy3-FYVE labeling at vertices ($P < 0.0001$; Fig. 6 B), which was not seen with the inactive analogue 7-OH-3NC (not depicted). Vacuolar fusion is inhibited by 3NC but not by 7-OH-3NC (Jun et al., 2005), suggesting that PLC activity is required for vacuole fusion but not for vertex enrichment of PI(3)P. The enhancement of PI(3)P vertex enrichment by LatB or 3NC, which block the late stages of fusion, suggests that PI(3)P vertex enrichment may be lost during or after fusion.

Lipids govern the vertex enrichment of fusion regulatory proteins

Because regulatory lipids depend on each other and on fusion proteins for vertex enrichment (Figs. 5 and 6), we asked whether fusion protein vertex enrichment may depend on regulatory lipids. We examined the effect of lipid ligands on vertex enrichment of Ypt7p, the SNAREs Vam7p, Vam3p, and Vti1p, and the HOPS subunit Vps33p. Ypt7p vertex enrichment is impervious to several protein-targeted inhibitors of fusion (Wang et al., 2003), yet was blocked by ENTH, C1b, FYVE, or filipin ($P < 0.0001$; Fig. 7 A). The inhibition of Ypt7p enrichment by FYVE contrasts with the previous finding that the PI(3)P ligand PX domain did not affect Ypt7p vertex accumulation (Wang et al., 2003). This may reflect a greater affinity of dimeric FYVE than monomeric PX for PI(3)P.

Published December 20, 2004

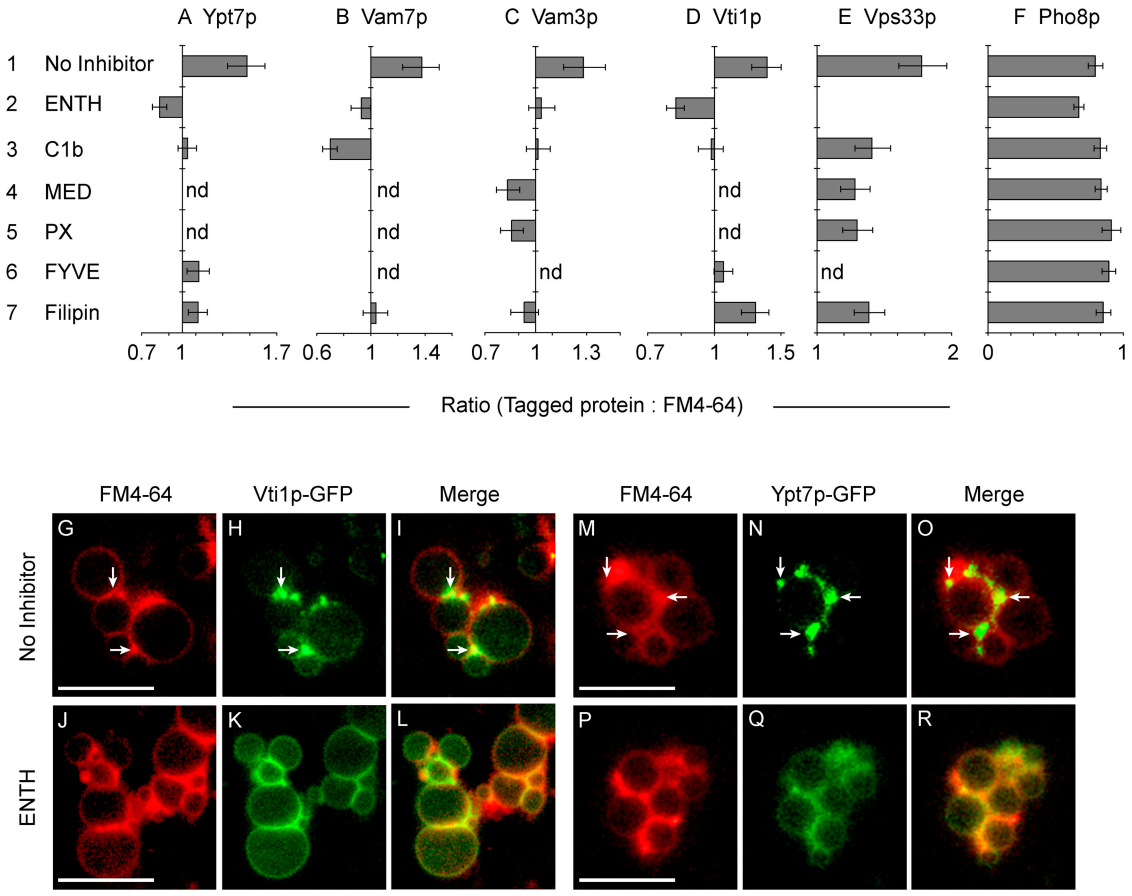

Figure 7. **Regulatory lipids control the vertex enrichment of Ypt7p, SNAREs, and HOPS.** Docking reactions using vacuoles from strains expressing GFP fusions to Ypt7p (A), Vam7p (B), Vam3p (C), Vti1p (D), Vps33p (E), or Pho8p (F) were treated with 30 μM ENTH, 10 μM MED, 10 μM C1b, 19 μM filipin, 25 μM PX, or 2 μM GST-FYVE and assayed for vertex enrichment. Reactions were incubated for 30 min at 27°C, placed on ice and labeled with FM4-64. Geometric mean values ± 95% confidence intervals of relative vertex enrichment are shown. (G–R) Fluorescent images of docked vacuoles containing GFP-Vti1p (G–L), or GFP-Ypt7p (M–R). Docking reactions bore no inhibitor (G–I and M–O) or 30 μM ENTH (J–L and P–R). G, J, M, and P show membrane staining with FM4-64. H, K, N, and Q show the distribution of GFP-Vti1p (H and K) or GFP-Ypt7p (N and Q). Merged images illustrate the enrichment of GFP-Vti1p (I) and Ypt7p (O) at vertices relative to outer membrane. ENTH treatment abolished the vertex enrichment of these proteins (L and R). Arrows are examples of vertices enriched in GFP-Vti1 (H and I) and GFP-Ypt7 (N and O) relative to outer membrane. Bars, 5 μm.

Because SNAREs accumulate at vertices (Wang et al., 2003), we examined the roles of regulatory lipids on this process. The PI(3)P ligands FYVE and PX displace Vam7p from membranes (Boeddinghaus et al., 2002) and hence from vertices (Wang et al., 2003). Vam7p vertex localization was also suppressed by ENTH, C1b or filipin ($P < 0.0001$; Fig. 7 B). Because these lipid ligands reduce PI(3)P enrichment at vertices (Fig. 5 A), and Vam7p binds directly to PI(3)P, the other regulatory lipids may largely affect Vam7p vertex enrichment through controlling PI(3)P vertex enrichment. Vam3p vertex enrichment (Wang et al., 2003) was blocked by each regulatory lipid ligand ($P < 0.01$; Fig. 7 C). As Vam3p forms a complex with Vam7p (Ungermann and Wickner, 1998; Ungermann et al., 1999), regulatory lipids may govern Vam3p vertex enrichment directly or through Vam7p. ENTH, C1b, and FYVE also inhibited Vti1p vertex enrichment ($P < 0.0001$; Fig. 7 D). Vti1p does not depend on Vam3p or Vam7p for its vertex enrichment (Wang et al., 2003). In accord with this divergent SNARE enrichment pathway, Vti1p enrichment was not significantly affected by filipin (Fig. 7 D) even though filipin abolished the vertex enrichment of Vam7p and Vam3p (Fig. 7, B and C). Lipid ligands also inhibited Vps33p vertex enrichment ($P < 0.01$; Fig. 7 E). Examples of specific protein enrichment at vertices, and ENTH blockage of enrichment, are shown in Fig. 7 (G–R).

As a control, we examined the effects of these ligands on the distribution of Pho8-GFP, a trans-membrane vacuolar protein. Pho8p is not involved in fusion and is evenly distributed on docked vacuoles (Wang et al., 2002). Simple displacement of proteins from vertices by lipid ligands would have depleted Pho8-GFP from vertices. Pho8-GFP was not significantly displaced from vertices by any of the lipid ligands (Fig. 7 F), indicating that the effects of lipid ligands on bona fide fusion protein enrichment are specific.

Enzymatic modification of regulatory lipids inhibits vertex ring assembly

To complement the above studies, we used lipid modifying enzymes. MTM-1, which inhibits fusion (Fig. 1 G), blocked Ypt7p vertex enrichment ($P < 0.00001$; Fig. 8 A). This mirrors

Published December 20, 2004

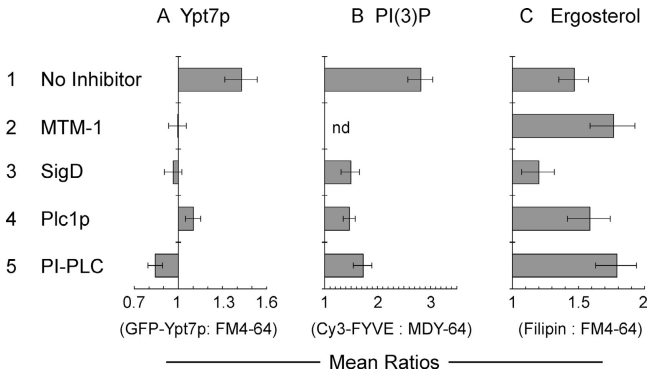

Figure 8. **Enzymatic modification of regulatory lipids inhibits vertex assembly.** Docking reactions (30 min, 27°C), using vacuoles containing GFP-Ypt7p (A) or vacuoles labeled with Cy3-FYVE to mark PI(3)P (B) or filipin to mark ergosterol (C), bore 1 μM MTM-1, 2 μM SigD, 1 U/ml PI-PLC, or 2.7 μM Plc1p. After incubation, reactions were placed on ice, counterstained with FM4-64 (A and C) or MDY-64 (B), and prepared for microscopic analysis. Geometric means ± 95% confidence intervals of the relative vertex enrichment are shown.

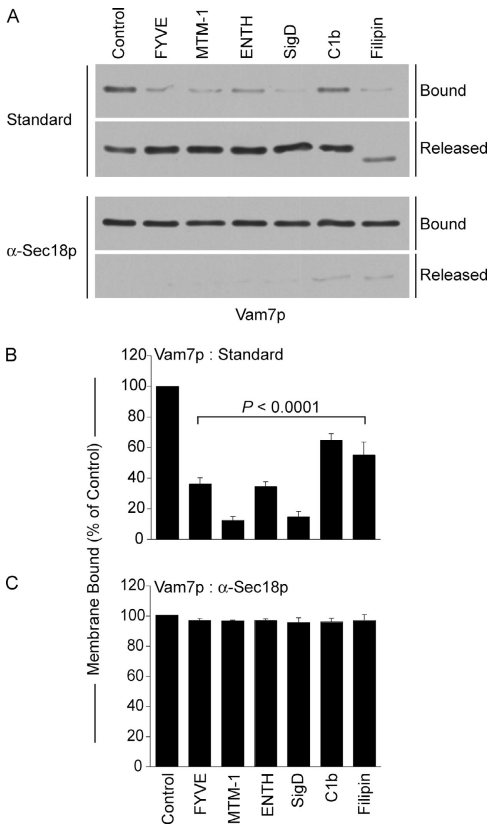

Figure 9. **Regulatory lipids are required for vacuolar association of Vam7p.** Vam7p association with vacuolar membranes was assayed by immunoblot in fusion reactions without inhibitor or with 2 μM GST-FYVE, 10 μM C1b, 19 μM filipin, 38 μM GST-ENTH, 2 μM SigD, or 1 μM MTM-1. Reactions were also performed in the presence of anti-Sec18p F_{ab} to inhibit priming. Fusion reactions were incubated for 90 min at 27°C, then fractionated into membrane pellets and supernatants by centrifugation (13,000 *g*, 15 min, 4°C). Membranes were resuspended in 30 μl PS buffer with protease inhibitors (1 μM leupeptin, 5 μM pepstatin and 0.1 μM pefabloc-SC). (A) Equal proportions of the pellet and supernatant fractions were mixed with SDS-loading buffer, resolved by SDS-PAGE, then transferred to nitrocellulose. (B and C) Quantitative analysis of membrane-bound Vam7p by Western blots. Data represent mean values ± SEM. Relative band intensities were measured using NIH Image 1.62 ($n = 4$).

the effect of FYVE domain on Ypt7p enrichment (Fig. 7 A), and confirms that PI(3)P is essential for Ypt7p vertex enrichment. MTM-1-mediated depletion of PI(3)P enhanced ergosterol enrichment ($P < 0.01$; Fig. 8 C), in accord with our observations using PX (Fig. 5 B). To complement our studies with ENTH on the role of $PI(4,5)P_2$, we used the PI 5-phosphatase SigD and $PI(4,5)P_2$ specific lipase Plc1p (Flick and Thorner, 1993). As for ENTH, SigD and Plc1p inhibited the vertex localization of Ypt7p and PI(3)P (Fig. 8, A and B; $P < 0.00001$). Interestingly, ergosterol vertex enrichment was inhibited by SigD ($P < 0.01$) but not by Plc1p (Fig. 8 C); the generation of DAG by Plc1p may slightly stimulate ergosterol enrichment, in accord with the modest decrease caused by C1b (Fig. 5 B). We also tested the role of unmodified PI. We have previously shown that the hydrolysis of PI by PI-PLC inhibits vacuole fusion (Mayer et al., 2000). This inhibition was relieved by the addition of $PI(4,5)P_2$ (ibid), suggesting that vacuolar PI primarily serves as a source for the synthesis of PI(4)P and $PI(4,5)P_2$. PI-PLC inhibited vertex enrichment of Ypt7p and PI(3)P ($P < 0.00001$; Fig. 8, A and B). The similarity of these results with those seen with Plc1p suggests that PI is needed for $PI(4,5)P_2$ synthesis for vacuole fusion.

Regulatory lipids modulate the vacuolar association of Vam7p

Lipids are important for the vacuole binding of perpheral membrane proteins. Soluble Vam7p can be released from vacuoles after priming (Sato et al., 1998; Ungermann and Wickner, 1998) and reassociates with vacuoles for docking (Ungermann et al., 2000). Vam7p lacks an apolar membrane anchor but has a PI(3)P-interacting PX domain (Cheever et al., 2001). Vam7p needs both PI(3)P and Ypt7p for stable membrane binding, after which it binds to Vam3p to promote fusion (Sato et al., 1998; Ungermann and Wickner, 1998; Ungermann et al., 2000).

Vacuole sedimentation allowed analysis of the Vam7p bound to the vacuole or remaining in the supernatant after standard fusion incubations without inhibitors or with lipid modifying enzymes or ligands (Fig. 9). Most of Vam7p is bound to vacuoles at the end of a fusion reaction. As reported (Boeddinghaus et al., 2002), FYVE domain caused Vam7p release. MTM-1 was equally effective at promoting Vam7p release. Although the Vamp7 PX domain has direct affinity for only PI(3)P (Cheever et al., 2001), the vacuole association of Vam7p was blocked by either ENTH, a $PI(4,5)P_2$ ligand, or by SigD, a $PI(4,5)P_2$ 5′phosphatase. C1b and Filipin also promote release of Vam7p. These data suggest that Ypt7p and PI(3)P may promote Vam7p association with vacuoles at vertices. Vam7p release was blocked when priming was inhibited by antibody to Sec18p (Fig. 9 C), showing that lipid ligands and modifying enzymes are only affecting Vam7p reassociation after it has been released from its associations with other integral membrane SNARE proteins by Sec18p-mediated priming.

Published December 20, 2004

Discussion

Our earlier studies explored the role of protein: protein interactions in protein enrichment at vertex microdomains (Wang et al., 2002, 2003). We now find that the regulatory lipids PI(3)P, $PI(4,5)P_2$, DAG and ergosterol are required for the assembly of vertex rings and for vacuole fusion. Each of these lipids is enriched at vertices, demonstrating that fusion catalysts operate within highly organized membrane domains. The localization of PI(3)P to vertices is not only dependent on other lipids, but is regulated by SNAREs. Moreover, the vertex enrichment of Ypt7p, HOPS and SNAREs as well as the membrane association of Vam7p (Boeddinghaus et al., 2002) are lipid-dependent. Ergosterol may contribute to vertex assembly by inhibiting the diffusion of enriched components in this microdomain and thereby slowing their exit from the vertex (Valdez-Taubas and Pelham, 2003). The fusion-regulatory lipids and proteins are mutually interdependent for their vertex enrichment.

Phosphoinositides are also required for other membrane trafficking steps and for the assembly of specific microdomains. Endocytosis (Li et al., 1995), and phagocytosis (Botelho et al., 2000; Marshall et al., 2001) depend on 3- and 4-phosphoinositides. The endosomal degradative pathway also requires PI(3)P. PI(3)P participates in the down-regulation of HGFR (Futter et al., 2001) and in phagolysosome biogenesis (Fratti et al., 2001). PI(3)P regulates the trafficking of hydrolytic enzymes from the Golgi to endosomes (Brown et al., 1995) and the formation of multivesicular bodies (Futter et al., 2001). Early endosome Rab5 recruits the PI3 kinase hVps34 (Christoforidis et al., 1999), forming PI(3)P and recruiting the tethering factor EEA1. Rab5 and EEA1 form a tethering complex that includes other Rab5 effectors, a SNARE and NSF (McBride et al., 1999). Rab5 and EEA1 colocalize in microdomains scattered throughout early endosomal membranes (McBride et al., 1999). Although all the components of the early endosome tethering complex are required for fusion, their coalescence into a single defined microdomain at the site of fusion has not been demonstrated. On the yeast vacuole, we find that regulatory lipids, SNAREs, Ypt7p and HOPS self-assemble in an interdependent manner into a domain which specifies the site of membrane fusion.

Phosphoinositide localization to sterol-rich microdomains

PI(3)P and ergosterol are interdependent for their vertex enrichment (Fig. 5, A and B). Although the role of PI(3)P in lipid domains has not been exhaustively studied, links between $PI(4,5)P_2$ function and sterol rich domains are well established. $PI(4,5)P_2$ concentrates in cholesterol-rich lipid domains in many cell types (Pike and Casey, 1996; Liu et al., 1998) and this can affect $PI(4,5)P_2$-interacting molecules. The link between PI function and sterols in higher eukaryotes has parallels with the regulation of vacuole fusion by lipids. In mammalian cells, extraction of cholesterol redistributes $PI(4,5)P_2$ (Yamashita et al., 2001) and inhibits EGFR signaling by blocking $PI(4,5)P_2$ turnover (Pike and Casey, 1996). The redistribution of $PI(4,5)P_2$ from lipid domains prevents PLC translocation from cytosol to membranes (Wang et al., 2001b), thereby inhibiting $PI(4,5)P_2$ turnover and the generation of IP_3 and DAG (Jang et al., 2001). The dependence of vacuole fusion on 4-phosphoinositides (Mayer et al., 2000), PLC activity (Jun et al., 2005), and sterols (Kato and Wickner, 2001) is consistent with the colocalization of phosphoinositides, DAG, and SNAREs to vacuolar microdomains.

Sterol and phosphoinositide interdependence at vertices is shown by the enrichment of each of these lipids and the sensitivity of this enrichment to ligands or modifiers of the other regulatory lipids. This model is supported by other studies showing that SNAREs are concentrated in cholesterol-dependent clusters that define docking and fusion sites for exocytosis (Lang et al., 2001). Furthermore the SNAREs SNAP-25 and Syntaxin 1 directly interact with caveolin 1, a resident of caveolae (Magga et al., 2002). Although these SNAREs are also present throughout the membrane, they are enriched in specific lipid microdomains. The SNARE synaptobrevin interacts with the cholesterol-binding protein synaptophysin, leading to enhanced synaptobrevin interactions with other SNAREs (Mitter et al., 2003). Disrupting lipid microdomains interferes with synaptobrevin/synaptophysin interactions and with synaptobrevin complex formation with other SNAREs (Mitter et al., 2003). In sum, SNARE-mediated membrane fusion requires lipid-regulated microdomains in other systems as well as in vacuoles.

Ypt7p functions near the beginning of the vertex ring assembly cascade (Wang et al., 2003). Although Ypt7p enrichment at vertices is resistant to all previously tested inhibitors of vacuole fusion (Wang et al., 2003), lipid ligands and modifiers block Ypt7p accumulation in this domain (Fig. 7 A and Fig. 8 A). Thus regulatory lipids, though not required for Ypt7p-dependent vesicle tethering (Fig. 2), are required for Ypt7p vertex enrichment. We postulate that the initial tethering events require Ypt7p action at the site of initial vacuole contact. This is followed by the establishment of a vertex ring of Ypt7p and the regulatory lipids. The assembly of a fully functional vertex ring is intricate, and our current understanding of the interdependence of lipids and proteins for ring assembly does not permit simple hierarchical models of their functions.

Materials and methods

Reagents

Reagents were dissolved in PS buffer (20 mM Pipes-KOH, pH 6.8, 200 mM sorbitol). MED (KKKKKRFSFKKSFKLSGFSFKKNKK) labeled with 5,6 carboxytetramethylrhodamine (excitation 546 nm, emission 576 nm) was from the Keck center (Yale). PSS-380 (excitation 380 nm, emission 440; a gift from A. Koulav, University of Notre Dame, IN) was dissolved in PS buffer at 1 mM. Anti-Vam3p F_{ab} (Wang et al., 2003), and anti-Sec18p F_{ab} (Mayer and Wickner, 1997) were described previously. Filipin III (excitation 337 nm, emission 480 nm; Sigma-Aldrich) was dissolved in DMSO at 1.16 mM. Jasplakinolide (Molecular Probes) and LatB (BIOMOL Research Laboratories, Inc.) were dissolved in DMSO at 10 mM. 3NC (a gift from E. Martegani, Universita di Milano, Italy) and 7-OH-3NC (a gift from D. Thakker, University of North Carolina, NC) were dissolved in DMSO at 3 and 6 mM, respectively. PI-PLC (from *Bacillus cereus*; Sigma-Aldrich) was dissolved in PS buffer with 125 mM KCl and 5 mM $MgCl_2$ and passed over a PD-10 column (Amersham Biosciences) in this buffer.

Recombinant proteins

C1b (plasmid a gift from A. Newton, University of California at San Diego, La Jolla, CA; Johnson et al., 2000), ENTH (plasmid a gift from P. De

Camilli, Yale University School of Medicine, New Haven, CT; Rosenthal et al., 1999), PX (Boeddinghaus et al., 2002), and tandem FYVE domain (plasmid a gift from H. Stenmark, The Norwegian Radium Hospital, Oslo, Norway; Gillooly et al., 2000) were produced as recombinant GST fusion proteins in *E. coli* as described. GST domains were removed by thrombin (Amersham Biosciences) or factor Xa (New England Biolabs, Inc.) cleavage according to each protease manufacturers' protocols and proteins were dialyzed into PS buffer with 125 mM KCl and 5 mM $MgCl_2$. Thrombin and factor Xa were removed from cleavage products by a p-aminobenzamidine-agarose (Sigma-Aldrich) column in PS buffer. FYVE and ENTH were labeled with Cy3 (excitation 546 nm, emission 570 nm; Research Organics) and C1b was labeled with Alexa488 (excitation 488 nm, emission 519 nm; Molecular Probes) according to the manufacturers' protocols. His_6-MTM-1 (plasmid a gift from J. Dixon, University of California at San Diego, La Jolla, CA; Taylor et al., 2000), his_6-SigD (plasmid a gift from B. Finlay, University of British Columbia, Vancouver, BC, Canada; Marcus et al., 2001), and his_6-Plc1p (Flick and Thorner, 1993) were prepared as described previously and dialyzed into PS buffer with 125 mM KCl and 5 mM $MgCl_2$. His_6-Sec17p and his_6-Sec18p were prepared as described previously (Haas and Wickner, 1996). His_6-Sec18p was further purified by gel filtration (Thorngren et al., 2004). Gdi1p (Garrett and Novick, 1995), his_6-Gyp1-46p (Wang et al., 2003) and IB2 (Slusarewicz et al., 1997) were prepared as described.

Vacuole isolation and in vitro fusion assay

Vacuoles were isolated from the yeast strains BJ3505 (Jones, 2002) and DKY6281 (Haas et al., 1994). Fusion reactions (30 μl) contained 3 μg of BJ3505 vacuoles with inactive pro-Pho8p (pro-alkaline phosphatase) but lacking the protease Pep4p, 3 μg of DKY6281 vacuoles containing Pep4p but lacking Pho8p, standard fusion reaction buffer (125 mM KCl, 5 mM $MgCl_2$, 20 mM Pipes-KOH, pH 6.8, 200 mM sorbitol), ATP regenerating system (1 mM ATP, 40 mM creatine phosphate, 0.1 mg/ml creatine kinase), 10 μM coenzyme A (Haas et al., 1995) and 930 nM IB2. After 90 min at 27°C, Pho8p activity was assayed in 250 mM Tris-Cl, pH 8.5, 0.4% Triton X-100, 10 mM $MgCl_2$, 1 mM *p*-nitrophenylphosphate. 1 U of fusion is 1 μmol *p*-nitrophenolate produced per min per μg of BJ3505 vacuoles. P-nitrophenolate absorbance was measured at 400 nm.

Vacuole docking assay

GFP-tagged strains and their use in docking assays were described previously (Wang et al., 2002, 2003). Isogenic strains containing the *ACT1* wild type and *act1-113* mutant alleles were a gift from D. Drubin (University of California at Berkeley, Berkeley, CA; Ayscough, 2000). Docking reactions (30 μl) contained 6 μg of vacuoles from DKY6281, unless otherwise noted, in 30 μl docking reaction buffer (100 mM KCl, 0.5 mM $MgCl_2$, 20 mM Pipes-KOH, pH 6.8, 200 mM sorbitol), ATP regenerating system (0.3 mM ATP, 6 mM creatine phosphate, 0.7 mg/ml creatine kinase), 20 μM coenzyme A, 930 nM IB2, 8 nM his_6-Sec18p and either no lipid ligand or 0.2 μM Cy3-FYVE, 0.6 μM ENTH, 5 μM filipin, 1 μM Alexa 488-C1b, 0.5 μM rhodamine-MED, or 2.5 μM PSS-380. After 30 min at 27°C, vacuoles bearing GFP-tagged proteins or labeled with filipin, PSS380, or Alexa488-C1b were place on ice and mixed with 0.7 μl of 160 μM FM4-64 for 2 min (3.7 μM final concentration; Molecular Probes). Vacuoles labeled with Cy3-FYVE domain or Cy3-ENTH domain were mixed with 1 μl of 16 μM MDY-64 (Molecular Probes) for 2 min. For Cy3-ENTH labeling, vacuoles were reisolated (5,220 *g*, 4°C, 5 min) at the end of the 30-min incubation to eliminate background fluorescence and resuspended in the original volume of PS buffer before labeling with MDY-64 and microscopic analysis. Vacuoles were then mixed with 50 μl of 0.6% agarose in PS buffer at 42°C, vortexed (3 s, medium setting), and 15 μl aliquots were mounted on slides and observed by fluorescence microscopy.

Images were acquired using a microscope (model BX51; Olympus) equipped with a 100W mercury arc lamp, Plan Apochromat 60× objective (1.4 NA) and a Sensicam QE CCD camera (Cooke). Images were acquired at 23°C without pixel binning. GFP proteins, Alexa488-C1b and MDY-64 images were acquired using an Endow GFP filter set (Chroma Technology Corp.). Cy3-FYVE, Cy3-ENTH, and FM4-64 images were acquired using a TRITC/DiI filter set (Chroma Technology Corp.). An XF06 filter set (Omega Optical, Inc.) was used to acquire filipin and PSS-380 images. Filter sets were housed in a motorized turret. FM4-64 and MDY-64 were used to focus fields and photobleaching was performed for 20 s between channels. Bleaching of specific probes (e.g., filipin), though minimal, was normalized by automated image acquisition using IP Lab software (Scanalytics). Image acquisition scripts, using fixed exposure times, first captured the nonspecific probe followed by the specific probe. This method ensures that any bleaching is uniform, and negates it as a factor in calculating intensity ratios. Images were processed and analyzed using Image/J software (NIH). For ratiometric quantitation, maximum pixel values for vertex, boundary and outer membrane were measured in each fluorescence channel. Every vertex and outer membrane within a vacuole cluster was measured. Vertex ratio values were normalized by dividing by the mean ratio values of outside edges. For each treatment, 15–20 clusters with 100–300 vertex sites were analyzed from multiple independent experiments. The data are presented from a representative experiment in each case. The range of mean ratio values reflect the daily variability of our vacuole preparation. However, this does not affect the responsiveness of vacuoles within each preparation to our panel of inhibitors.

Statistical analysis of vertex enrichment experiments used JMP 5 (SAS Institute, Inc.). Ratio data were log transformed before analysis to yield near-normal distributions with comparable variances. Ratio means and 95% confidence intervals were analyzed using one-way ANOVAs for each lipid ligand and GFP-protein fusion. Significant differences in vertex enrichment were determined using *t* test and corrected for multiple comparisons using the Dunn-Sidak method (Sokal and Rohlf, 1994). P-values less than 0.05 were considered significant.

We thank Drs. P. De Camilli, J. Dixon, D. Drubin, B. Finlay, A. Koulav, H. Martegani, A. Newton, H. Stenmark, and D. Thakker for reagents.

This work was supported by a grant from the National Institute of General Medical Sciences. R.A. Fratti is supported by a postdoctoral fellowship from the Helen Hay Whitney Foundation. A.J. Merz was supported by National Institute of Arthritis and Musculoskeletal and Skin Diseases training grant AR07576-09.

Submitted: 13 September 2004
Accepted: 8 November 2004

References

Ayscough, K.R. 2000. Endocytosis and the development of cell polarity in yeast require a dynamic F-actin cytoskeleton. *Curr. Biol.* 10:1587–1590.

Ayscough, K.R., J. Stryker, N. Pokala, M. Sanders, P. Crews, and D.G. Drubin. 1997. High rates of actin filament turnover in budding yeast and roles for actin in establishment and maintenance of cell polarity revealed using the actin inhibitor latrunculin-A. *J. Cell Biol.* 137:399–416.

Boeddinghaus, C., A.J. Merz, and C. Ungermann. 2002. A cycle of Vam7p release from and PtdIns 3-P-dependent rebinding to the yeast vacuole is required for homotypic vacuole fusion. *J. Cell Biol.* 157:79–90.

Botelho, R.J., M. Teruel, R. Dierckman, R. Anderson, A. Wells, J.D. York, T. Meyer, and S. Grinstein. 2000. Localized biphasic changes in phosphatidylinositol-4,5-bisphosphate at sites of phagocytosis. *J. Cell Biol.* 151:1353–1368.

Brown, W.J., D.B. DeWald, S.D. Emr, H. Plutner, and W.E. Balch. 1995. Role for phosphatidylinositol 3-kinase in the sorting and transport of newly synthesized lysosomal enzymes in mammalian cells. *J. Cell Biol.* 130:781–796.

Chavrier, P., and B. Goud. 1999. The role of ARF and Rab GTPases in membrane transport. *Curr. Opin. Cell Biol.* 11:466–475.

Cheever, M.L., T.K. Sato, T. de Beer, T.G. Kutateladze, S.D. Emr, and M. Overduin. 2001. Phox domain interaction with PtdIns(3)P targets the Vam7 t-SNARE to vacuole membranes. *Nat. Cell Biol.* 3:613–618.

Christoforidis, S., M. Miaczynska, K. Ashman, M. Wilm, L. Zhao, S.C. Yip, M.D. Waterfield, J.M. Backer, and M. Zerial. 1999. Phosphatidylinositol-3-OH kinases are Rab5 effectors. *Nat. Cell Biol.* 1:249–252.

Eitzen, G., N. Thorngren, and W. Wickner. 2001. Rho1p and Cdc42p act after Ypt7p to regulate vacuole docking. *EMBO J.* 20:5650–5656.

Eitzen, G., L. Wang, N. Thorngren, and W. Wickner. 2002. Vacuole-bound actin regulates homotypic membrane fusion. *J. Cell Biol.* 158:669–679.

Fasshauer, D., H. Otto, W.K. Eliason, R. Jahn, and A.T. Brunger. 1997. Structural changes are associated with soluble N-ethylmaleimide-sensitive fusion protein attachment protein receptor complex formation. *J. Biol. Chem.* 272:28036–28041.

Flick, J.S., and J. Thorner. 1993. Genetic and biochemical characterization of a phosphatidylinositol-specific phospholipase C in *Saccharomyces cerevisiae*. *Mol. Cell. Biol.* 13:5861–5876.

Fratti, R.A., J.M. Backer, J. Gruenberg, S. Corvera, and V. Deretic. 2001. Role of phosphatidylinositol 3-kinase and Rab5 effectors in phagosomal biogenesis and mycobacterial phagosome maturation arrest. *J. Cell Biol.* 154:631–644.

Fukuda, R., J.A. McNew, T. Weber, F. Parlati, T. Engel, W. Nickel, J.E. Rothman, and T.H. Sollner. 2000. Functional architecture of an intracellular membrane t-SNARE. *Nature.* 407:198–202.

Futter, C.E., L.M. Collinson, J.M. Backer, and C.R. Hopkins. 2001. Human VPS34 is required for internal vesicle formation within multivesicular endosomes. *J. Cell Biol.* 155:1251–1264.

Garrett, M.D., and P.J. Novick. 1995. Expression, purification, and assays of Gdi1p from recombinant *Escherichia coli*. *Methods Enzymol.* 257:232–240.

Gerst, J.E. 1999. SNAREs and SNARE regulators in membrane fusion and exocytosis. *Cell. Mol. Life Sci.* 55:707–734.

Gillooly, D.J., I.C. Morrow, M. Lindsay, R. Gould, N.J. Bryant, J.M. Gaullier, R.G. Parton, and H. Stenmark. 2000. Localization of phosphatidylinositol 3-phosphate in yeast and mammalian cells. *EMBO J.* 19:4577–4588.

Guo, W., F. Tamanoi, and P. Novick. 2001. Spatial regulation of the exocyst complex by Rho1 GTPase. *Nat. Cell Biol.* 3:353–360.

Haas, A., and W. Wickner. 1996. Homotypic vacuole fusion requires Sec17p (yeast alpha-SNAP) and Sec18p (yeast NSF). *EMBO J.* 15:3296–3305.

Haas, A., B. Conradt, and W. Wickner. 1994. G-protein ligands inhibit in vitro reactions of vacuole inheritance. *J. Cell Biol.* 126:87–97.

Haas, A., D. Scheglmann, T. Lazar, D. Gallwitz, and W. Wickner. 1995. The GTPase Ypt7p of *Saccharomyces cerevisiae* is required on both partner vacuoles for the homotypic fusion step of vacuole inheritance. *EMBO J.* 14:5258–5270.

Higgs, H.N., and T.D. Pollard. 2000. Activation by Cdc42 and PIP(2) of Wiskott-Aldrich syndrome protein (WASp) stimulates actin nucleation by Arp2/3 complex. *J. Cell Biol.* 150:1311–1320.

Inoue, S., and K.R. Spring. 1997. Video Microscopy: The Fundamentals (The Language of Science). Plenum, New York. 741 pp.

Jahn, R. 2000. Sec1/Munc18 proteins: mediators of membrane fusion moving to center stage. *Neuron.* 27:201–204.

Jahn, R., and T.C. Sudhof. 1999. Membrane fusion and exocytosis. *Annu. Rev. Biochem.* 68:863–911.

Jang, I.H., J.H. Kim, B.D. Lee, S.S. Bae, M.H. Park, P.G. Suh, and S.H. Ryu. 2001. Localization of phospholipase C-gamma1 signaling in caveolae: importance in EGF-induced phosphoinositide hydrolysis but not in tyrosine phosphorylation. *FEBS Lett.* 491:4–8.

Johnson, J.E., J. Giorgione, and A.C. Newton. 2000. The C1 and C2 domains of protein kinase C are independent membrane targeting modules, with specificity for phosphatidylserine conferred by the C1 domain. *Biochemistry.* 39:11360–11369.

Jones, E.W. 2002. Vacuolar proteases and proteolytic artifacts in *Saccharomyces cerevisiae*. *Methods Enzymol.* 351:127–150.

Jun, Y., R.A. Fratti, and W. Wickner. 2005. Diacylglycerol and its formation by phospholipase C regulate Rab- and SNARE-dependent yeast vacuole fusion. *J. Biol. Chem.* In press.

Kato, M., and W. Wickner. 2001. Ergosterol is required for the Sec18/ATP-dependent priming step of homotypic vacuole fusion. *EMBO J.* 20: 4035–4040.

Koulov, A.V., K.A. Stucker, C. Lakshmi, J.P. Robinson, and B.D. Smith. 2003. Detection of apoptotic cells using a synthetic fluorescent sensor for membrane surfaces that contain phosphatidylserine. *Cell Death Differ.* 10:1357–1359.

Lang, T., D. Bruns, D. Wenzel, D. Riedel, P. Holroyd, C. Thiele, and R. Jahn. 2001. SNAREs are concentrated in cholesterol-dependent clusters that define docking and fusion sites for exocytosis. *EMBO J.* 20:2202–2213.

Li, G., C. D'Souza-Schorey, M.A. Barbieri, R.L. Roberts, A. Klippel, L.T. Williams, and P.D. Stahl. 1995. Evidence for phosphatidylinositol 3-kinase as a regulator of endocytosis via activation of Rab5. *Proc. Natl. Acad. Sci. USA.* 92:10207–10211.

Liu, Y., L. Casey, and L.J. Pike. 1998. Compartmentalization of phosphatidylinositol 4,5-bisphosphate in low- density membrane domains in the absence of caveolin. *Biochem. Biophys. Res. Commun.* 245:684–690.

Magga, J.M., J.G. Kay, A. Davy, N.P. Poulton, S.M. Robbins, and J.E. Braun. 2002. ATP dependence of the SNARE/caveolin 1 interaction in the hippocampus. *Biochem. Biophys. Res. Commun.* 291:1232–1238.

Marcus, S.L., M.R. Wenk, O. Steele-Mortimer, and B.B. Finlay. 2001. A synaptojanin-homologous region of Salmonella typhimurium SigD is essential for inositol phosphatase activity and Akt activation. *FEBS Lett.* 494:201–207.

Marshall, J.G., J.W. Booth, V. Stambolic, T. Mak, T. Balla, A.D. Schreiber, T. Meyer, and S. Grinstein. 2001. Restricted accumulation of phosphatidylinositol 3-kinase products in a plasmalemmal subdomain during Fcγ receptor-mediated phagocytosis. *J. Cell Biol.* 153:1369–1380.

Mayer, A., and W. Wickner. 1997. Docking of yeast vacuoles is catalyzed by the Ras-like GTPase Ypt7p after symmetric priming by Sec18p (NSF). *J. Cell Biol.* 136:307–317.

Mayer, A., W. Wickner, and A. Haas. 1996. Sec18p (NSF)-driven release of Sec17p (alpha-SNAP) can precede docking and fusion of yeast vacuoles. *Cell.* 85:83–94.

Mayer, A., D. Scheglmann, S. Dove, A. Glatz, W. Wickner, and A. Haas. 2000. Phosphatidylinositol 4,5-bisphosphate regulates two steps of homotypic vacuole fusion. *Mol. Biol. Cell.* 11:807–817.

McBride, H.M., V. Rybin, C. Murphy, A. Giner, R. Teasdale, and M. Zerial. 1999. Oligomeric complexes link Rab5 effectors with NSF and drive membrane fusion via interactions between EEA1 and syntaxin 13. *Cell.* 98:377–386.

McLaughlin, S., J. Wang, A. Gambhir, and D. Murray. 2002. PIP(2) and proteins: interactions, organization, and information flow. *Annu. Rev. Biophys. Biomol. Struct.* 31:151–175.

Mitter, D., C. Reisinger, B. Hinz, S. Hollmann, S.V. Yelamanchili, S. Treiber-Held, T.G. Ohm, A. Herrmann, and G. Ahnert-Hilger. 2003. The synaptophysin/synaptobrevin interaction critically depends on the cholesterol content. *J. Neurochem.* 84:35–42.

Morton, W.M., K.R. Ayscough, and P.J. McLaughlin. 2000. Latrunculin alters the actin-monomer subunit interface to prevent polymerization. *Nat. Cell Biol.* 2:376–378.

Muller, O., D.I. Johnson, and A. Mayer. 2001. Cdc42p functions at the docking stage of yeast vacuole membrane fusion. *EMBO J.* 20:5657–5665.

Muller, O., H. Neumann, M.J. Bayer, and A. Mayer. 2003. Role of the Vtc proteins in V-ATPase stability and membrane trafficking. *J. Cell Sci.* 116: 1107–1115.

Nichols, B.J., C. Ungermann, H.R. Pelham, W.T. Wickner, and A. Haas. 1997. Homotypic vacuolar fusion mediated by t- and v-SNAREs. *Nature.* 387:199–202.

Peters, C., P.D. Andrews, M.J. Stark, S. Cesaro-Tadic, A. Glatz, A. Podtelejnikov, M. Mann, and A. Mayer. 1999. Control of the terminal step of intracellular membrane fusion by protein phosphatase 1. *Science.* 285:1084–1087.

Peters, C., and A. Mayer. 1998. Ca^{2+}/calmodulin signals the completion of docking and triggers a late step of vacuole fusion. *Nature.* 396:575–580.

Peters, C., M.J. Bayer, S. Buhler, J.S. Andersen, M. Mann, and A. Mayer. 2001. Trans-complex formation by proteolipid channels in the terminal phase of membrane fusion. *Nature.* 409:581–588.

Pike, L.J., and L. Casey. 1996. Localization and turnover of phosphatidylinositol 4,5-bisphosphate in caveolin-enriched membrane domains. *J. Biol. Chem.* 271:26453–26456.

Price, A., D. Seals, W. Wickner, and C. Ungermann. 2000. The docking stage of yeast vacuole fusion requires the transfer of proteins from a cis-SNARE complex to a Rab/Ypt protein. *J. Cell Biol.* 148:1231–1238.

Roberts, R.L., M.A. Barbieri, K.M. Pryse, M. Chua, J.H. Morisaki, and P.D. Stahl. 1999. Endosome fusion in living cells overexpressing GFP-rab5. *J. Cell Sci.* 112:3667–3675.

Rosenthal, J.A., H. Chen, V.I. Slepnev, L. Pellegrini, A.E. Salcini, P.P. Di Fiore, and P. De Camilli. 1999. The epsins define a family of proteins that interact with components of the clathrin coat and contain a new protein module. *J. Biol. Chem.* 274:33959–33965.

Rozelle, A.L., L.M. Machesky, M. Yamamoto, M.H. Driessens, R.H. Insall, M.G. Roth, K. Luby-Phelps, G. Marriott, A. Hall, and H.L. Yin. 2000. Phosphatidylinositol 4,5-bisphosphate induces actin-based movement of raft-enriched vesicles through WASP-Arp2/3. *Curr. Biol.* 10:311–320.

Sato, T.K., T. Darsow, and S.D. Emr. 1998. Vam7p, a SNAP-25-like molecule, and Vam3p, a syntaxin homolog, function together in yeast vacuolar protein trafficking. *Mol. Cell. Biol.* 18:5308–5319.

Seeley, E.S., M. Kato, N. Morgolis, W. Wickner, and G. Eitzen. 2002. Genomic analysis of homotypic vacuole fusion. *Mol. Biol. Cell.* 13:782–794.

Seki, K., F.S. Sheu, and K.P. Huang. 1996. Binding of myristoylated alanine-rich protein kinase C substrate to phosphoinositides attenuates the phosphorylation by protein kinase C. *Arch. Biochem. Biophys.* 326:193–201.

Slusarewicz, P., Z. Xu, K. Seefeld, A. Haas, and W.T. Wickner. 1997. I2B is a small cytosolic protein that participates in vacuole fusion. *Proc. Natl. Acad. Sci. USA.* 94:5582–5587.

Sokal, R.R., and F.J. Rohlf. 1994. Biometry: The Principles and Practice of Statistics in Biological Research. W.H. Freeman, New York. 859 pp.

Taylor, G.S., T. Maehama, and J.E. Dixon. 2000. Inaugural article: myotubularin, a protein tyrosine phosphatase mutated in myotubular myopathy, dephosphorylates the lipid second messenger, phosphatidylinositol 3-phosphate. *Proc. Natl. Acad. Sci. USA.* 97:8910–8915.

TerBush, D.R., T. Maurice, D. Roth, and P. Novick. 1996. The Exocyst is a multiprotein complex required for exocytosis in *Saccharomyces cerevisiae*. *EMBO J.* 15:6483–6494.

Thorngren, N., K.M. Collins, R.A. Fratti, W. Wickner, and A.J. Merz. 2004. A soluble SNARE drives rapid docking, bypassing ATP and Sec17/18p for vacuole fusion. *EMBO J.* 23:2765–2776.

Tisi, R., P. Coccetti, S. Banfi, and E. Martegani. 2001. 3-Nitrocoumarin is an efficient inhibitor of budding yeast phospholipase-C. *Cell Biochem. Funct.* 19:229–235.

Ungermann, C., and W. Wickner. 1998. Vam7p, a vacuolar SNAP-25 homolog,

is required for SNARE complex integrity and vacuole docking and fusion. *EMBO J.* 17:3269–3276.

Ungermann, C., G.F. von Mollard, O.N. Jensen, N. Margolis, T.H. Stevens, and W. Wickner. 1999. Three v-SNAREs and two t-SNAREs, present in a pentameric cis-SNARE complex on isolated vacuoles, are essential for homotypic fusion. *J. Cell Biol.* 145:1435–1442.

Ungermann, C., A. Price, and W. Wickner. 2000. A new role for a SNARE protein as a regulator of the Ypt7/Rab-dependent stage of docking. *Proc. Natl. Acad. Sci. USA.* 97:8889–8891.

Valdez-Taubas, J., and H.R. Pelham. 2003. Slow diffusion of proteins in the yeast plasma membrane allows polarity to be maintained by endocytic cycling. *Curr. Biol.* 13:1636–1640.

Wang, J., A. Arbuzova, G. Hangyas-Mihalyne, and S. McLaughlin. 2001a. The effector domain of myristoylated alanine-rich C kinase substrate binds strongly to phosphatidylinositol 4,5-bisphosphate. *J. Biol. Chem.* 276:5012–5019.

Wang, L., C. Ungermann, and W. Wickner. 2000. The docking of primed vacuoles can be reversibly arrested by excess Sec17p (alpha-SNAP). *J. Biol. Chem.* 275:22862–22867.

Wang, L., E.S. Seeley, W. Wickner, and A.J. Merz. 2002. Vacuole fusion at a ring of vertex docking sites leaves membrane fragments within the organelle. *Cell.* 108:357–369.

Wang, L., A.J. Merz, K.M. Collins, and W. Wickner. 2003. Hierarchy of protein assembly at the vertex ring domain for yeast vacuole docking and fusion. *J. Cell Biol.* 160:365–374.

Wang, X.J., H.J. Liao, A. Chattopadhyay, and G. Carpenter. 2001b. EGF-dependent translocation of green fluorescent protein-tagged PLC-gamma1 to the plasma membrane and endosomes. *Exp. Cell Res.* 267: 28–36.

Wang, Y.X., E.J. Kauffman, J.E. Duex, and L.S. Weisman. 2001c. Fusion of docked membranes requires the armadillo repeat protein Vac8p. *J. Biol. Chem.* 276:35133–35140.

Wickner, W., and A. Haas. 2000. Yeast homotypic vacuole fusion: a window on organelle trafficking mechanisms. *Annu. Rev. Biochem.* 69:247–275.

Yamashita, T., T. Yamaguchi, K. Murakami, and S. Nagasawa. 2001. Detergent-resistant membrane domains are required for mast cell activation but dispensable for tyrosine phosphorylation upon aggregation of the high affinity receptor for IgE. *J. Biochem. (Tokyo).* 129:861–868.